Computer simulation of vapor–liquid equilibria of linear quadrupolar fluids. Departures from the principle of corresponding states

Benito Garzón, Santiago Lago,[a] and Carlos Vega
Departamento de Química Física, Facultad de Ciencias Químicas, Universidad Complutense de Madrid, 28040 Madrid, Spain

Enrique de Miguel and Luis F. Rull
Departamento de Física Atómica Molecular y Nuclear, Universidad de Sevilla, Aptdo 1065, Sevilla 41080, Spain

(Received 22 February 1994; accepted 23 May 1994)

Vapor–liquid equilibria of different quadrupolar linear Kihara fluids have been studied, by using the Gibbs ensemble Monte Carlo technique. Coexistence curves for fluids with elongations $L^*=L/\sigma=0.3$, 0.6, and 0.8 and different quadrupoles are given. We analyze the effect of quadrupole moment on critical properties. Quadrupole moment increases the critical temperature, pressure, and density. The magnitude of the increase depends on both anisotropy and quadrupole moment. A new way of reducing the quadrupole is proposed, so that the variation of critical properties due to the quadrupole follows a universal behavior. Quadrupole provokes deviations from the principle of corresponding states. A broadening of the coexistence curve is observed due to the quadrupole. The quadrupole moment increases the slope of the vapor pressure curve vs temperature inverse. Simulation data are used to describe vapor–liquid equilibria of carbon dioxide. Good agreement between simulation and experiment is achieved.

I. INTRODUCTION

Among the most important and useful concepts in the development of thermophysical property correlations is the principle of corresponding states, enunciated by van der Waals in 1873. According to this principle, all fluids obeying an equation of state with two parameters should follow the same equation when reduced by their critical magnitudes. The molecular ground for this principle was established by Pitzer[1] and Guggenheim.[2] Although this principle was a very useful tool to describe the behavior of nearly spherical substances with not too low molecular-weight, substantial deviations from this principle were observed for some types of fluids.[3]

For low molecular weight fluids, quantum corrections are important in the description of their properties, as is the case of helium. More commonly, deviations from the principle of corresponding states arise from nonspherical forces as, for instance, short-range repulsive forces arising from molecular shape or long-range attractive forces arising from multipole moments.

There have been many empirical attempts to account for such deviations by including a third parameter that is a measure of the molecular anisotropy. The most widely used is the so-called *acentric factor*, first introduced by Pitzer *et al.*[4] These attempts have been very useful in providing an empirical description of the behavior of fluids, but a *molecular understanding* of deviations from the principle of corresponding states is still needed.

An early theoretical attempt to study the influence of molecular anisotropy and multipolar forces of simple fluids upon deviations from the principle of corresponding states was made by Cook and Rowlinson.[5] Several theories have been developed since then, which have accounted for the role of shape or/and polarity on departures from the principle of corresponding states. The effect of a dipole or quadrupole moment on the behavior of a spherical fluid is well known due to the studies made by Pople, Gubbins *et al.*, and Stell *et al.* using perturbation theory and conventional computer simulation experiments.[11–14] Recent Gibbs ensemble computer simulations made by Stapleton *et al.*[15] and Smit and co-workers[16–18] completed that study.

More recently, the effect of molecular shape upon deviations from the principle of corresponding states has been studied. Perturbation theories developed for two-center Lennard-Jones fluids by Monson and co-workers[19,20] and Fischer *et al.*,[21] and the improved perturbation theory proposed by Vega and Lago[22] for Kihara fluids have given a clear picture of how the molecular shape modifies the coexistence properties of a fluid. Furthermore, studies of the vapor–liquid equilibria by using computer simulation in the Gibbs ensemble carried out by de Miguel *et al.*[23,24] for the Gay–Berne model and by ourselves for linear Kihara fluids[25] have completed the study of the influence of molecular anisotropy upon deviations from the principle of corresponding states.

However, little effort has been dedicated to study the role of both shape and polarity onto departures from the principle of corresponding states. Lupkowski and Monson[26] have studied the effect of dipole moment on vapor–liquid equilibria of linear molecules using a perturbation theory for site–site fluids. Their results have been recently confirmed by Gibbs ensemble simulations made by Dubey *et al.*.[27] However, the effect of a quadrupole moment upon the vapor–liquid equilibria (VLE), critical properties, and departures from the principle of corresponding states of a molecular fluid remains unknown.

The goal of this work is to study the effect of quadrupole

[a]Author to whom correspondence should be addressed.

 0021-9606/94/101(5)/4166/11/$6.00 © 1994 American Institute of Physics

moment on the vapor–liquid equilibria, critical properties, and deviations from the principle of corresponding states of a linear molecular fluid. We have studied fluids consisting of linear molecules interacting with a Kihara potential having an embedded point quadrupole. Such a fluid provides a simple model for such important fluids as N_2, Cl_2, and CO_2. Moreover, the phase diagram of this model when no quadrupole is present is already known from a previous work.[25] Conclusions of this study concerning the influence of the quadrupole moment on the phase diagram can be probably extended to any linear molecular fluid model, as the two-center Lennard-Jones. In fact, both nonpolar linear Kihara and nonpolar two-center Lennard-Jones models present the same departures from the principle of corresponding states due to the molecular shape.[25,27] We expect this to be still true when multipolar forces are present.

We have used the Gibbs ensemble simulation technique to obtain the coexistence curve of a quadrupolar linear Kihara fluid, for three different values of molecular elongation and two different values of quadrupole for each elongation. To our knowledge, these are the first simulation data of the vapor–liquid equilibria of quadrupolar molecular fluids. These results may be useful to check some recently developed theories for multipolar molecular fluids, as the perturbation theory proposed by Boublík for dipolar and quadrupolar Kihara fluids.[28–30]

The scheme of the paper is as follows. In Sec. II we describe the molecular model and simulation method. In Sec. III we present and discuss the obtained results, the influence of the quadrupole upon the coexistence curve, critical properties and vapor pressures, as well as the universal behavior of critical properties with the quadrupole as a new way of reducing the quadrupole moment is used. Application of simulation data to the thermodynamic description of a real fluid is also shown. Conclusions are shown in Sec. IV.

II. SIMULATION METHOD

We consider a quadrupolar linear fluid consisting of rods of length L with an embedded point quadrupole Q, interacting through a potential given by

$$u(r,\omega_1,\omega_2)=u^K(r,\omega_1,\omega_2)+u^{QQ}(r,\omega_1,\omega_2), \tag{1}$$

where r is the distance between the centers of mass of the molecules and $\omega_i \equiv \{\theta_i,\phi_i\}$ stands for the polar angles of molecule i with respect to a reference frame having its polar axis aligned along the center of mass separation vector, $\mathbf{r}$. u^K is the Kihara potential,[31] given by

$$u^K(r,\omega_1,\omega_2)=4\epsilon\left\{\left[\frac{\sigma}{\rho(r,\omega_1,\omega_2)}\right]^{12}-\left[\frac{\sigma}{\rho(r,\omega_1,\omega_2)}\right]^{6}\right\} \tag{2}$$

and u^{QQ} is the quadrupole–quadrupole potential, given by

$$u^{QQ}(r,\omega_1,\omega_2)=\frac{3Q^2}{4r^5}[1-5(c_1^2+c_2^2+3c_1^2c_2^2) +2(s_1s_2c_{12}-4c_1c_2)^2]. \tag{3}$$

In Eq. (2), $\rho(r,\omega_1,\omega_2)$ is the shortest distance between the molecular cores (see Fig. 1), ϵ is an energetic parameter and σ a size parameter. In Eq. (3), Q is the quadrupole moment, $c_i=\cos\theta_i$, $s_i=\sin\theta_i$, and $c_{12}=\cos(\phi_2-\phi_1)$.

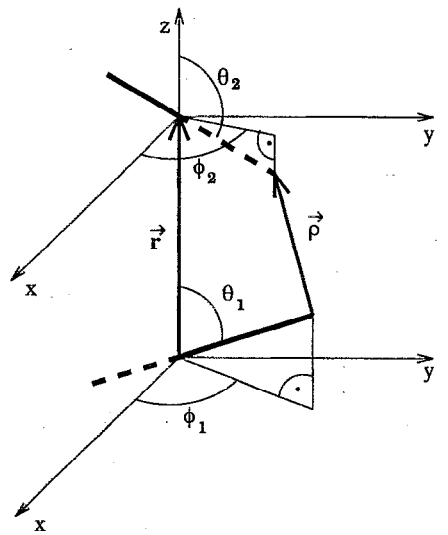

FIG. 1. Shortest distance ρ between two linear rods of length L.

The Kihara potential is a reliable model for describing thermodynamic behavior of fluids. Second virial coefficient can be determined analitically for this potential,[32] so that vapor properties can be easily described. Kihara used this potential successfully in the study of solid structures.[33] Its application to the study of liquid phase has been made by using thermodynamic perturbation theories,[34–37] and it has been shown that it constitutes a good effective pair potential for real substances.[38,39] When $L=0$ and $Q=0$, the potential function given by Eqs. (1)–(3) reduces to the well-known Lennard-Jones potential.

Evaluation of the Kihara potential requires the calculation of the shortest distance between two linear rods. This seems to be a very time consuming task, but very efficient algorithms for its determination are available,[39–42] so that the computer time expended in the evaluation of the Kihara potential between two linear rods is similar to the time required to evaluate the two-center Lennard-Jones interaction between two molecules.

To determine the VLE of quadrupolar linear Kihara molecules we shall use the Gibbs ensemble Monte Carlo (GEMC) simulation technique. This method, developed by Panagiotopoulos,[43] allows the direct determination of the coexistence curve, simulating simultaneously both phases. This technique involves three steps. In the first one, a conventional *NVT* MC simulation step is performed in the vapor and in the liquid. The second step consists in an attempt of changing the volume of one of the simulation boxes by ΔV and by $-\Delta V$ in the other. The acceptance of this move is taken from the *NPT* MC method assuming equal pressures for both phases. In the last step, in order to keep the same chemical potential in both phases, a number of particle exchanges between the boxes is attempted, with a probability given by μVT MC simulation. A more detailed description of this method can be found in the original papers.[43,44]

We have obtained VLE of linear quadrupolar Kihara fluids of reduced length $L^*=L/\sigma=0.3$, 0.6, and 0.8 using the Gibbs ensemble technique. From a previous work,[25] we know the coexistence curve of these systems for $Q=0$. We used 512 molecules. At temperatures close to the critical point, the initial configuration was taken from an α-N_2 lattice, with 256 molecules in each box. At lower temperatures, final configurations from previous runs were used. The interaction was truncated at $\rho=3\sigma$ and long range corrections were applied by assuming uniform fluid beyond the cutoff. Formulas for the evaluation of long-range contribution to the internal energy and pressure of a Kihara fluid can be found in Ref. 45. Additional formula for the chemical potential can be easily derived. By assuming uniform fluid beyond the cutoff, the contribution of the quadrupole to the long range corrections vanishes.[46,47] To obtain a point of the coexistence curve, we performed 3000–5000 steps for equilibration plus 4000–8000 steps for averages. A step consists of an attempt of moving each particle in both phases, followed by an attempt of changing the volume and N_{ex} attempts of exchanging particles between the simulation boxes. Acceptance ratio was kept in the range 30%–60% and N_{ex} was chosen to get an exchange ratio of 1%–3%. We obtained VLE for $T \geqslant 0.75\ T_c$. We were not able to obtain phase equilibria when $T<0.75\ T_c$. This is because at low temperatures the density of a liquid in equilibrium with its vapor is very high, and the acceptance probability in the particle exchange step becomes extremely low. This seems to be a general problem when the GEMC method is applied to molecular fluids. To obtain a point of the coexistence curve, we need about 15 h of cpu time on a Silicon Graphics workstation.

The critical temperature, T_c^*, density, n_c^*, and pressure, P_c^* were estimated by fitting the simulation data to the expressions

$$\frac{n_l^*+n_g^*}{2}=a+bT^*, \tag{4}$$

$$n_l^*-n_g^*=c\left(1-\frac{T^*}{T_c^*}\right)^{\beta}, \tag{5}$$

$$\ln P^*=d+\frac{e}{T^*}, \tag{6}$$

where n_l^* and n_g^* are the liquid and vapor reduced densities ($n^*=n\sigma^3$, with n being the number density), $T^*=kT/\epsilon$ is the reduced temperature, and $P^*=P\sigma^3/\epsilon$ is the reduced vapor pressure. Equation (4) is the rectilinear diameters law.[2] In Eq. (5), we assumed a critical exponent $\beta=1/3$, close to the universal value given by the Group Renormalization Theory.[48] Equation (6) is the Clausius–Clapeyron equation for the vapor pressure.[49]

The three studied elongations ($L^*=0.3$, 0.6, 0.8) correspond approximately to the molecular anisotropy presented by N_2, Cl_2, and CO_2, respectively. These substances show a nonzero quadrupole moment. For $L^*=0$ the molecular model reduces to a quadrupolar Lennard-Jones potential for which GEMC data are available.[15,16]

III. RESULTS AND DISCUSSION

We have obtained the coexistence curve of linear Kihara fluids at the mentioned elongations and for two different values of the reduced quadrupole for each elongation. The reduced quadrupole, Q^{*2}, is defined as

$$Q^{*2}=\frac{Q^2}{\epsilon\sigma^5}. \tag{7}$$

Studied systems are $L^*=0.3$ and $Q^{*2}=0.75$, 1.5; $L^*=0.6$ and $Q^{*2}=1.18$, 2.35; and $L^*=0.8$ and $Q^{*2}=1.5$, 3.0.

In Tables I–III the results of simulations are presented. Reduced temperatures, vapor and liquid densities and pressures on the coexistence curve are given. The estimated errors were obtained from the standard deviations over blocks of 100 steps. For some temperatures, several independent runs were performed.

In Figs. 2, 3, and 4 we compare the results of this work for $L^*=0.3$, 0.6, and 0.8, respectively, with the previous data obtained by ourselves for the nonpolar Kihara model. Table IV shows the critical properties (temperature, density, pressure, packing fraction, and compressibility factor) as estimated from the simulation results making use of Eqs. (4)–(6). Results for quadrupolar Lennard-Jones fluids from Refs. 15 and 16 are also presented, as well as Lennard-Jones critical properties from Ref. 50.

These results show that the critical temperature increases significantly as the reduced quadrupole Q^{*2} increases. This connects with the idea often discussed in General Chemistry textbooks that for two molecules with similar van der Waals forces the presence of a multipole moment in one of them increases substancially the boiling temperature.[51,52] This is a consequence of the increase of the critical temperature due to the quadrupole moment. The effect of quadrupole upon the critical density is the same, but less significant. The critical pressure also increases with the quadrupole moment. No significant effect of quadrupole moment on the critical compressibility factor is observed, due to the statistical errors. A similar behavior of critical properties was observed for the quadrupolar Lennard-Jones fluid. From Figs. 2–4 we can also affirm that, for a given temperature, orthobaric densities are greater as reduced quadrupole increases. This is in part a consequence of the increase of the critical temperature.

In Fig. 5 we show the variation of the reduced critical temperature, ΔT_c^*, defined as

$$\Delta T_c^*=T_c^*(Q^*)-T_c^*(Q^*=0) \tag{8}$$

and critical packing fraction, η_c,

$$\eta_c=n_cV_m \tag{9}$$

with the reduced quadrupole moment, at different values of L^*. In Eq. (8), $T_c^*(Q^*)$ is the reduced critical temperature of the system with reduced quadrupole moment Q^* and $T_c^*(Q^*=0)$ stands for the reduced critical temperature of the nonpolar system with the same elongation. In Eq. (9), V_m is the molecular volume

$$V_m=\frac{\pi}{6}\sigma^3(1+1.5L^*). \tag{10}$$

TABLE I. Results for phase coexistence properties of linear quadrupolar Kihara fluids of $L^*=L/\sigma=0.3$ and $Q^{*2}=Q^2/(\epsilon\sigma^5)=0.75$ and 1.5. All thermodynamic properties are given in reduced units. The number in parentheses indicate the uncertainty in units of the last decimal digit; 0.472(10) means 0.472±0.010.

T^*	n_g^*	P_g^*	n_l^*	P_l^*
		$Q^{*2}=0.75$		
0.85	0.014 36(37)	0.001 6(55)	0.533 8(89)	0.07(11)
0.875	0.018 31(44)	0.003 9(32)	0.518 7(72)	0.050(76)
0.9	0.018 10(72)	0.019 0(20)	0.509 4(74)	0.036(83)
0.925	0.025 75(66)	0.010 43(66)	0.503 0(81)	0.007(90)
0.95	0.025 4(21)	0.017 3(31)	0.479 4(93)	0.009(51)
0.975	0.033 2(15)	0.025 45(55)	0.472(10)	0.026(27)
1	0.039 (23)	0.029 4(15)	0.455(12)	0.032(29)
1.025	0.044 5(19)	0.033 5(12)	0.432(18)	0.030(45)
1.05	0.054 6(60)	0.039 7(27)	0.420(21)	0.036(27)
1.075	0.068 8(26)	0.048 2(19)	0.412(19)	0.045(31)
1.1	0.085 1(62)	0.053 4(18)	0.389(21)	0.056(26)
1.11	0.089 4(79)	0.057 5(36)	0.348(48)	0.056(22)
1.12	0.087 9(74)	0.058 6(36)	0.353(24)	0.055(75)
1.13	0.104(11)	0.063 7(45)	0.344(45)	0.063(24)
1.14	0.105 1(70)	0.066 4(42)	0.348(32)	0.068(27)
		$Q^{*2}=1.5$		
1.05	0.021 0(21)	0.015 8(48)	0.511(10)	−0.010(78)
1.05	0.025 1(16)	0.016 7(63)	0.519 0(80)	0.024(78)
1.1	0.032 1(15)	0.024 9(67)	0.488 8(80)	0.025(26)
1.1	0.038 55(34)	0.032 0(24)	0.498 2(89)	0.059(35)
1.125	0.038 4(27)	0.032 7(17)	0.470 5(92)	0.029 6(31)
1.15	0.043 41(36)	0.037 4(26)	0.457 3(82)	0.038(39)
1.175	0.052 8(69)	0.043 5(38)	0.439(14)	0.031(33)
1.2	0.058 0(85)	0.047 0(51)	0.415(18)	0.044(31)
1.2	0.062 3(99)	0.049 5(55)	0.420(12)	0.045(31)
1.225	0.077(14)	0.059 3(65)	0.407(17)	0.062(30)
1.23	0.078 4(79)	0.060 7(55)	0.408(13)	0.063(21)
1.235	0.098 8(65)	0.067 8(58)	0.396(22)	0.069(27)
1.25	0.105 5(17)	0.070 4(85)	0.386(19)	0.067(27)
1.26	0.108 1(84)	0.072 5(58)	0.380(19)	0.072(26)
1.27	0.123 4(59)	0.077 9(59)	0.363(28)	0.071(32)
1.275	0.136(21)	0.075 0(85)	0.337(21)	0.070(21)
1.28	0.115(24)	0.077 6(85)	0.295(47)	0.073(14)

From Fig. 5 it may be concluded that the effect of the same value of reduced quadrupole on critical properties is greater as elongation of molecules is lower. This corresponds to the intuitive idea that the effect of a given quadrupole on the phase diagram of a fluid increases as the molecule turns to be more spherical. However, to compare the influence of quadrupole moment onto coexistence properties between molecular fluids of different elongations and quadrupoles it seems to be necessary to define *corresponding states* that would take into account the anisotropy. Thus, Bohn *et al.*[46] have defined approximate *corresponding states* for quadrupolar diatomic fluids by using *pseudocritical* properties that implicitly include the effect of elongation. Kihara and Koide[33] have also defined corresponding states between fluids of different anisotropy reducing the quadrupole moment with the critical volume and temperature of the fluid. For quadrupolar spherical fluids, the usual way of reducing the quadrupole moment is made with the definition of Eq. (7), that is, by using the diameter of the molecule, σ, as the factor that takes into account the shape of the molecule. In fact, we can rewrite Eq. (7) as

$$Q^{*2}=\frac{Q^2}{\epsilon[V_m/(\pi/6)]^{5/3}}=\left(\frac{\pi}{6}\right)^{5/3}\frac{Q^2}{\epsilon V_m^{5/3}}. \tag{11}$$

When molecules have a nonspherical shape, instead of using the diameter of the molecule to reduce the quadrupole, we could use the volume of the molecule as the factor that would appear in the definition of reduced quadrupole.

In this work, we suggest a different choice of reducing the quadrupole moment for molecules with different elongation. Following the form of Eq. (11), we shall define a *reduced density of quadrupole* as

$$\mathbb{Q}^2=\frac{Q^2}{\epsilon V_m^{5/3}}. \tag{12}$$

Usefulness of $\mathbb{Q}^2$ will depend on whether Eq. (12) allows a principle of corresponding states (even in an approximate way) between quadrupolar fluids of different anisotropy; that is, whether a fluid of $L^*=0.3$ and $Q^{*2}=1.5$ ($\mathbb{Q}^2=2.4$) may be compared with a fluid of $L^*=0.8$ and $Q^{*2}=3$ ($\mathbb{Q}^2=2.4$), since their *reduced density of quadrupole* is the same. In Table IV, values of $\mathbb{Q}^2$ are given for all systems.

TABLE II. Results for phase coexistence properties of linear quadrupolar Kihara fluids of $L^*=L/\sigma=0.6$ and $Q^{*2}=Q^2/(\epsilon\sigma^5)=1.18$ and 2.35.

T^*	n_g^*	P_g^*	n_l^*	P_l^*
		$Q^{*2}=1.18$		
0.825	0.014 56(35)	−0.000 44(62)	0.392 3(55)	0.016(62)
0.85	0.016 7(13)	0.011 78(81)	0.377 4(79)	0.009(28)
0.875	0.020 4(13)	0.014 43(73)	0.369 2(66)	0.011(24)
0.9	0.027 9(31)	0.018 9(19)	0.355 0(68)	0.018(23)
0.925	0.029 3(12)	0.020 49(77)	0.342(12)	0.015(32)
0.95	0.035 9(26)	0.024 6(14)	0.328(11)	0.023(30)
1	0.056 4(32)	0.035 5(19)	0.294(20)	0.028(29)
1.015	0.069 1(32)	0.040 3(25)	0.288(25)	0.031(28)
1.025	0.063 1(47)	0.039 5(25)	0.270(21)	0.039(13)
1.04	0.081 2(73)	0.046 0(32)	0.243(34)	0.044(15)
		$Q^{*2}=2.35$		
0.95	0.014 41(29)	0.015 5(29)	0.402 4(46)	0.02(11)
1	0.022 1(10)	0.017 68(88)	0.384 0(92)	0.021(33)
1.05	0.031 2(28)	0.024 4(20)	0.355 5(87)	0.020(33)
1.1	0.054 6(43)	0.037 6(27)	0.337 6(66)	0.036(66)
1.125	0.066 7(41)	0.043 1(30)	0.314(15)	0.047(23)
1.15	0.065 1(45)	0.045 2(28)	0.289(19)	0.045(19)
1.165	0.075 9(77)	0.049 4(38)	0.256(25)	0.047(21)
1.175	0.090(12)	0.053 3(48)	0.250(36)	0.049(25)

Figure 6 shows that the raise of critical temperature and packing fraction with increasing Q^2 follow now a universal curve regardless of the value of L^*. Thus, the common idea quoted above that the effect of the quadrupole on the phase diagram of a fluid increases as the molecule turns to be more spherical must be more carefully considered. Now, we can affirm that the role of molecular elongation in the increase of critical properties is secondary, at least in the studied range

TABLE III. Results for phase coexistence properties of linear quadrupolar Kihara fluids of $L^*=L/\sigma=0.8$ and $Q^{*2}=Q^2/(\epsilon\sigma^5)=1.5$ and 3.

T^*	n_g^*	P_g^*	n_l^*	P_l^*
		$Q^{*2}=1.5$		
0.775	0.009 75(17)	0.005 4(35)	0.345 2(56)	0.033(79)
0.8	0.015 1(13)	0.001 4(21)	0.338 2(33)	0.034(49)
0.825	0.014 7(11)	0.010 2(17)	0.323 0(46)	0.005(33)
0.85	0.016 8(17)	0.012 8(22)	0.308 9(55)	0.002(23)
0.85	0.018 39(76)	0.012 47(53)	0.313 7(56)	0.006(24)
0.875	0.027 0(10)	0.016 2(35)	0.304 5(94)	0.015(26)
0.9	0.033 1(65)	0.020 5(29)	0.296 0(67)	0.024(28)
0.9	0.036 2(31)	0.021 7(16)	0.295 2(63)	0.025(19)
0.925	0.038 4(32)	0.023 7(14)	0.277 9(90)	0.024(16)
0.95	0.053 6(59)	0.030 1(33)	0.267 1(75)	0.029(13)
0.965	0.052 6(49)	0.030 9(28)	0.250 9(99)	0.031(13)
0.975	0.058 2(59)	0.032 8(22)	0.236(14)	0.031(14)
0.985	0.068(11)	0.035 0(42)	0.232(16)	0.033(14)
1	0.089(13)	0.039 9(47)	0.227(17)	0.042(13)
1.01	0.091(13)	0.041 6(45)	0.205(29)	0.042(11)
		$Q^{*2}=3$		
0.925	0.013 01(39)	−0.001(10)	0.347 1(48)	0.037(90)
0.95	0.018 8(24)	0.014 0(15)	0.337 3(43)	0.19(21)
0.975	0.020 2(10)	0.015 51(86)	0.326 4(75)	0.015(25)
1	0.021 78(94)	0.016 78(84)	0.311 6(56)	0.014(24)
1.025	0.029 5(20)	0.021 7(14)	0.304 7(97)	0.021(22)
1.05	0.041 8(51)	0.027 5(27)	0.297 6(87)	0.028(23)
1.075	0.039 7(33)	0.028 3(18)	0.272(11)	0.026(17)
1.1	0.054 1(37)	0.035 3(22)	0.260(10)	0.034(20)
1.125	0.070 6(40)	0.042 7(42)	0.246(17)	0.044(20)
1.127 5	0.083 9(49)	0.044 9(47)	0.239(11)	0.045(20)
1.135	0.075 1(55)	0.044 2(37)	0.227(19)	0.047(18)
1.145	0.087 5(46)	0.046 6(44)	0.232(17)	0.051(15)

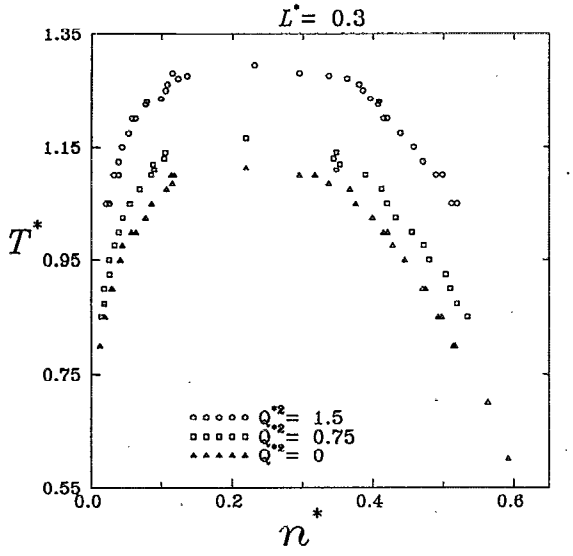

FIG. 2. Vapor–liquid coexistence densities for quadrupolar Kihara fluids of $L^*=L/\sigma=0.3$. The results are given in reduced units, $T^*=kT/\epsilon$ and $n^*=n\sigma^3$. Data corresponding to a reduced quadrupole $Q^{*2}=Q^2/(\epsilon\sigma^5)=1.5$ are plotted with circles. Squares correspond to $Q^{*2}=0.75$. Triangles represent data for the nonpolar system of Ref. 25.

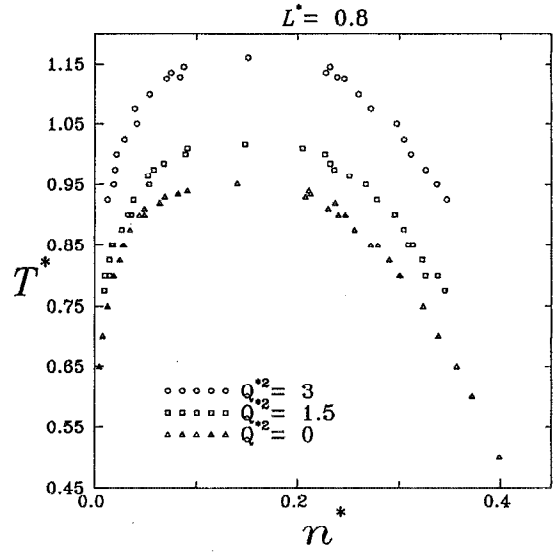

FIG. 4. Same as in Fig. 2, but for $L^*=L/\sigma=0.8$. Data corresponding to a reduced quadrupole $Q^{*2}=Q^2/(\epsilon\sigma^5)=3$ are plotted with circles. Squares correspond to $Q^{*2}=1.5$. Triangles represent data of nonpolar system of Ref. 25.

of elongations. Moreover, we cannot say in Fig. 6 whether points corresponding to $L^*=0$ are above or below points of $L^*=0.8$, due to the unaccuracy of data. The universality of the curve of Fig. 6 supports our choice of $\mathbb{Q}^2$ for comparing fluids with different L^* and Q^*. This universality occurs when ΔT_c is reduced with ϵ/k.

The consequences of the universality shown in Fig. 6 are quite interesting. For instance, if the critical temperature for a linear Kihara fluid with elongation L^* and $Q^*=0$ is known, T_c may be predicted for any value of Q^{*2} ($\mathbb{Q}^2$), by reading ΔT_c in Fig. 6 and adding that to the critical temperature of the nonpolar fluid.

In Fig. 7 we show the coexistence curve, when the temperature and density are reduced by their corresponding critical parameters, for the three values of L^*. Although the results shown in Fig. 7 are quite sensitive to errors in the determination of critical properties, so that caution is needed, we observe that the trend is a broadening of the VLE coexistence curve due to the quadrupole moment. This effect is moderate. Results of Refs. 15 and 16 show the same trend for a Lennard-Jones fluid. GEMC simulations of Stockmayer fluids also show departures from the principle of corresponding states.[17,18] Monson and co-workers[26,27] show a similar broadening of the coexistence curve for a dipolar two-center

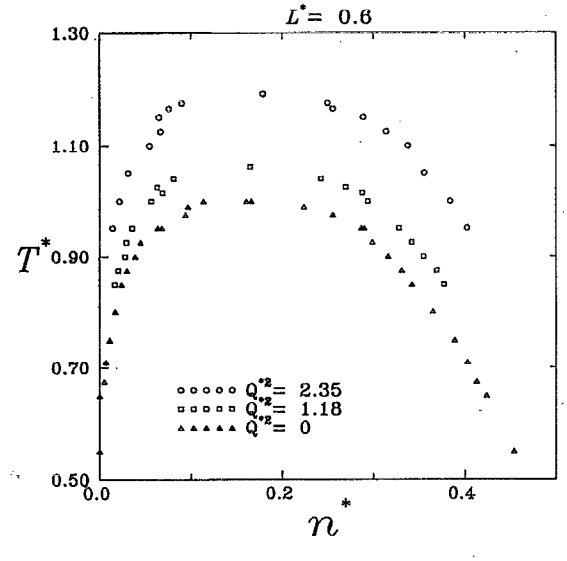

FIG. 3. Same as in Fig. 2, but for $L^*=L/\sigma=0.6$. Data corresponding to a reduced quadrupole $Q^{*2}=Q^2/(\epsilon\sigma^5)=2.35$ are plotted with circles. Squares correspond to $Q^{*2}=1.18$. Triangles represent data of nonpolar system of Ref. 25.

TABLE IV. Critical properties of simulated systems.

L^*	Q^{*2}	$\mathbb{Q}^2$	T_c^*	n_c^*	P_c^*	η_c	Z_c
0	0	0	1.310[a]	0.314[a]	0.126[a]	0.164[a]	0.306[a]
	0.40	1.2	1.40[b]	0.33[b]	0.14[b]	0.17[b]	0.30[b]
	0.81	2.4	1.54[b]	0.34[b]	0.16[b]	0.18[b]	0.31[b]
0.3	0	0	1.114(12)	0.219(6)	0.073(10)	0.166(5)	0.30(4)
	0.75	1.2	1.163(27)	0.220(16)	0.078(21)	0.167(12)	0.31(8)
	1.5	2.4	1.296(34)	0.231(31)	0.089(27)	0.175(24)	0.30(9)
0.6	0	0	1.000(12)	0.161(5)	0.051(10)	0.160(5)	0.32(6)
	1.18	1.2	1.061(22)	0.164(13)	0.050(12)	0.164(13)	0.29(7)
	2.35	2.4	1.192(19)	0.179(31)	0.058(25)	0.178(31)	0.27(12)
0.8	0	0	0.952(11)	0.140(3)	0.038(8)	0.161(4)	0.29(6)
	1.5	1.2	1.014(13)	0.147(14)	0.044(12)	0.169(16)	0.30(8)
	3	2.4	1.157(27)	0.152(16)	0.049(20)	0.175(18)	0.28(11)

[a]Result obtained by using the data of Ref. 50.
[b]Results obtained by interpolation of data from Refs. 15 and 16.

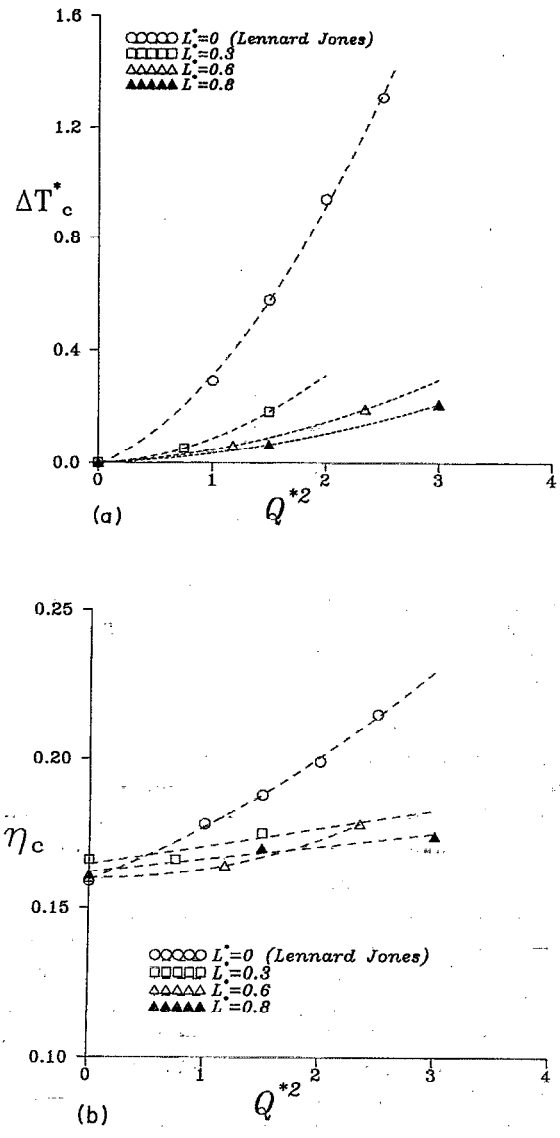

FIG. 5. (a) Increase of the reduced critical temperature [see Eq. (8) in the text] as a function of the reduced quadrupole for $L^*=0$ (circles) (results obtained from Refs. 15 and 16), $L^*=0.3$ (squares), $L^*=0.6$ (open triangles), and $L^*=0.8$ (filled triangles). (b) Critical packing fraction ($\eta=nV_m$, with V_m being the molecular volume) as a function of the reduced quadrupole. Symbols are as in (a). Lines are plotted as a guide to the eye.

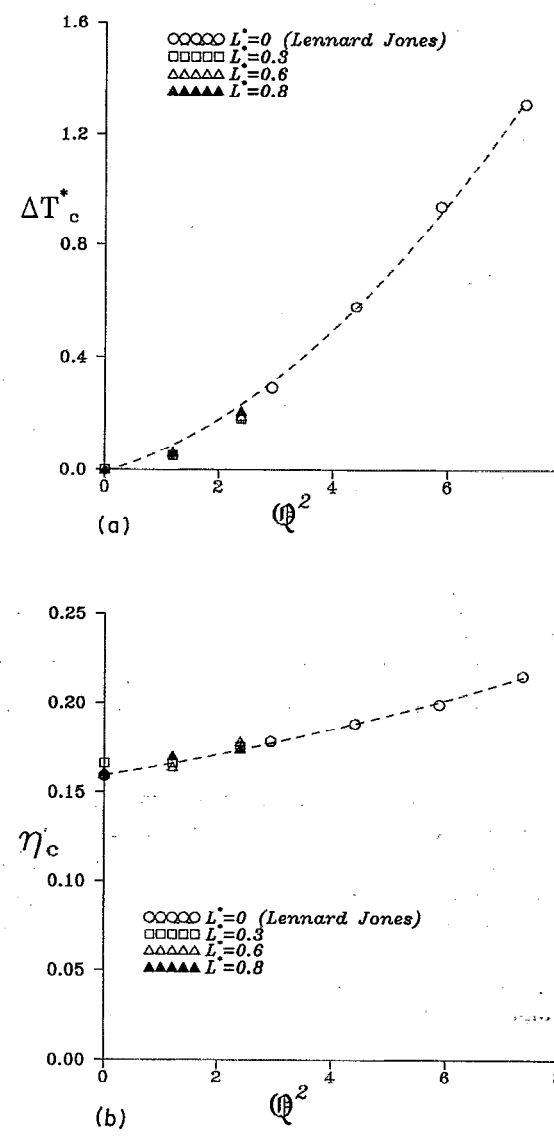

FIG. 6. (a) Increase of the reduced critical temperature as a function of the *reduced density of quadrupole*, $\mathbb{Q}^2$ [see Eq. (11) in the text] for $L^*=0$ (circles) (results obtained from Refs. 15 and 16), $L^*=0.3$ (squares), $L^*=0.6$ (white triangles), and $L^*=0.8$ (filled triangles). (b) Critical packing fraction ($\eta=nV_m$, with V_m being the molecular volume) as a function of the reduced density of quadrupole. Symbols are as in (a). Lines are plotted as a guide to the eye.

Lennard-Jones fluid when the dipole moment is increased. In conclusion, it seems that multipoles provoke a broadening of VLE coexistence densities, when plotted in terms of critical units.

The effect of quadrupole moment on the vapor pressure is shown in Fig. 8, at two values of L^*. The quadrupole moment decreases the vapor pressure at a given temperature. The same effect is observed for the quadrupolar Lennard-Jones fluid.[15,16] According to the Clausius–Clapeyron equation, which becomes accurate at low temperatures, the slope of a $\ln P^*$ vs $1/T^*$ plot is related with the vaporization enthalpy by

$$\frac{d\ln P^*}{d1/T^*}=-\frac{\Delta H_v}{N\epsilon}=-\Delta H_v^*. \tag{13}$$

In Fig. 8 the logarithm of the reduced vapor pressure is represented vs inverse of reduced temperature, at two different elongations, and different reduced quadrupoles. We can conclude that since the slope of the lines is almost constant that implies, from Eq. (13), that at low temperatures ΔH_v^* is relatively constant. We see from Fig. 8 that ΔH_v^* increases as the quadrupole is increased. This confirms the idea (widely quoted on text books of Chemistry) that vaporization enthalpy increases when molecules have a multipole moment.[51,52]

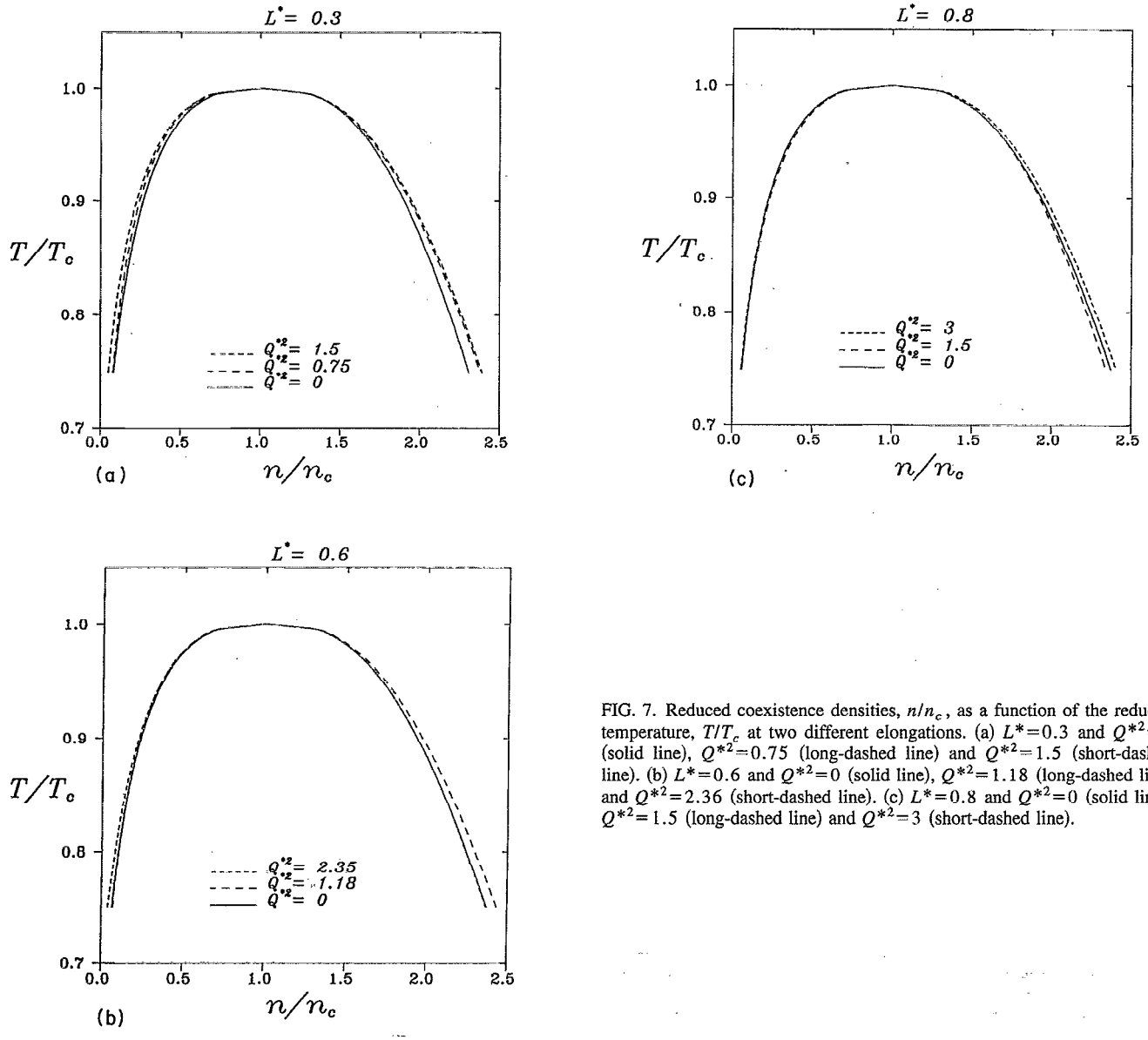

FIG. 7. Reduced coexistence densities, n/n_c, as a function of the reduced temperature, T/T_c at two different elongations. (a) $L^*=0.3$ and $Q^{*2}=0$ (solid line), $Q^{*2}=0.75$ (long-dashed line) and $Q^{*2}=1.5$ (short-dashed line). (b) $L^*=0.6$ and $Q^{*2}=0$ (solid line), $Q^{*2}=1.18$ (long-dashed line) and $Q^{*2}=2.36$ (short-dashed line). (c) $L^*=0.8$ and $Q^{*2}=0$ (solid line), $Q^{*2}=1.5$ (long-dashed line) and $Q^{*2}=3$ (short-dashed line).

Departures from the principle of corresponding states in the vapor pressure due to the quadrupole are illustrated by plots of $\ln(P/P_c)$ vs T_c/T. This is represented in Fig. 9 for $L^*=0.3$ and 0.8. We have also represented the vapor pressure of a Lennard-Jones fluid, taken from Ref. 50. Thus, it can be observed the effect that both shape and quadrupole exert upon deviations from corresponding states for vapor pressure. The slope (in absolute value) of the $\ln(P/P_c)$ curve increases with the molecular anisotropy (i.e., compare $L^*=0$, $Q^{*2}=0$ with $L^*=0.3$, $Q^{*2}=0$) as well as with the quadrupole moment (i.e., compare $L^*=0.3$, $Q^{*2}=0$ with $L^*=0.3$, $Q^{*2}=1.5$). Although these results should be taken with care due to difficulties in determining accurately critical magnitudes, we believe this trend to be correct.

In Chemical Engineering a measure of deviations upon corresponding states is given by the acentric factor, ω, defined as[4]

$$\omega=-\log\left(\frac{P}{P_c}\right)_{T=0.7T_c}-1 \tag{14}$$

related with the slope of the $\ln(P/P_c)$ vs T_c/T plot. Calculated acentric factors for simulated systems are shown in Table V. Results are affected by a considerable statistical error, due to errors made in the determination of critical pressure and temperature and vapor pressures at $T=0.7\ T_c$. Nevertheless, we can conclude that both anisotropy and quadrupole increase the magnitude of the acentric factor. Table V illustrates the variation of the acentric factor with $\mathbb{Q}^2$ for fixed L^*. We may suggest that this variation follows a universal behavior, when plotted vs $\mathbb{Q}^2$ for different L^*, but this effect is screened by the statistical error in ω. Therefore, no conclusion about this point is possible at this moment. It

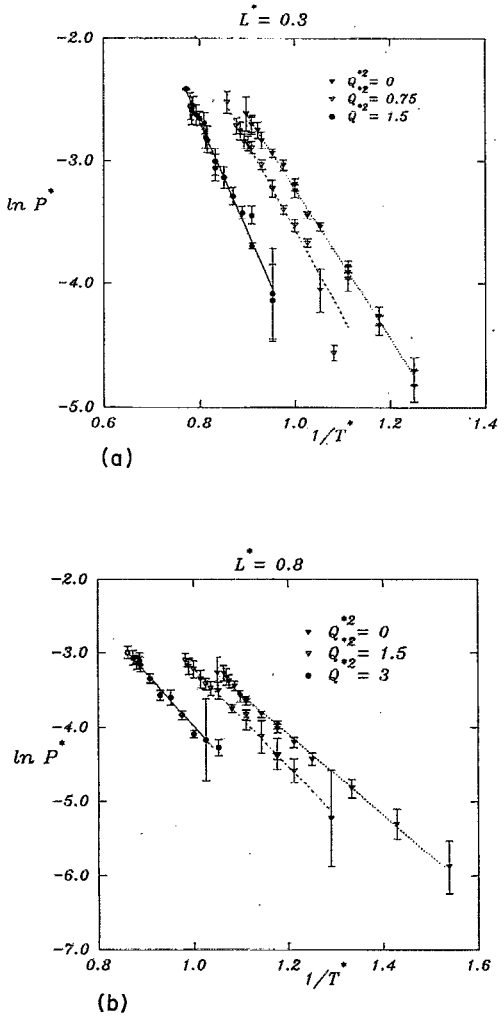

FIG. 8. Logarithm of the reduced vapor pressures, $P^*=P\sigma^3/\epsilon$, vs the inverse of reduced temperature, $1/T^*=1/(kT/\epsilon)$, for two different elongations. (a) $L^*=0.3$ and $Q^{*2}=0$ (filled triangles), $Q^{*2}=0.75$ (open triangles), and $Q^{*2}=1.5$ (filled circles). (b) $L^*=0.8$ and $Q^{*2}=0$ (filled triangles), $Q^{*2}=1.5$ (open triangles), and $Q^{*2}=3$ (filled circles).

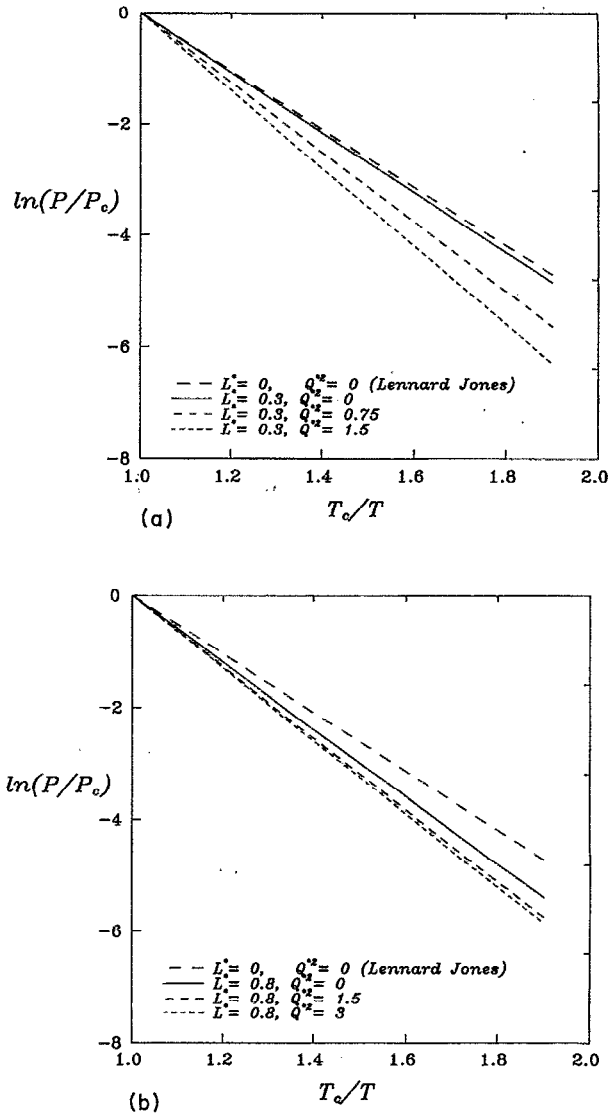

FIG. 9. Reduced vapor pressures as a function of the inverse of reduced temperature for $L^*=0$, 0.3, and 0.8. (a) Results for (from top to bottom) $L^*=0$ and $Q^{*2}=0$, and $L^*=0.3$ with $Q^{*2}=0$, 0.75, and 1.5. (b) Results for (from the top to the bottom) $L^*=0$ and $Q^{*2}=0$, and $L^*=0.8$ with $Q^{*2}=0$, 1.5, and 3.

seems that the GEMC method cannot give values of ω with the accuracy that is obtained from experimental measurements.

Until now, we have applied GEMC simulations to calculate VLE of a model fluid. It is possible to calculate the coexistence curve of a real fluid if adequate parameters of the Kihara potential are taken. Boublík has recently studied thermodynamic properties of carbon dioxide by using perturbation theory for quadrupolar Kihara fluids.[28] He considered CO_2 as a linear rod of $L^*=0.8118$ and $Q^{*2}=2.6$. A good description of VLE of CO_2 can also be obtained by using the GEMC data of the system with $L^*=0.8$ and $Q^{*2}=3$. Critical temperature and density obtained from simulations were fit to the experimental critical temperature and density of carbon dioxide,[53] as

$$\sigma(A)=\left[\frac{n_c^*10\,000}{n_c^{\exp}(\mathrm{mol/l})6.023}\right]^{1/3}, \tag{15}$$

$$\epsilon/k(K)=\frac{T_c^{\exp}(K)}{T_c^*}. \tag{16}$$

Quadrupolar Kihara parameters calculated in this way are $\epsilon/k=262.93$ K and $\sigma=2.878$ A. The quadrupole mo-

TABLE V. Acentric factors for the simulated systems.

Q^2	$L^*=0$	$L^*=0.3$	$L^*=0.6$	$L^*=0.8$
0	0.02[a]	0.00(12)	0.15(16)	0.11(12)
1.2	0.07[b]	0.17(20)	0.11(18)	0.19(20)
2.4	0.11[b]	0.30(24)	0.13(30)	0.22(28)

[a]Result obtained by using formulas of Ref. 50.
[b]Results obtained by interpolation of data from Refs. 15 and 16.

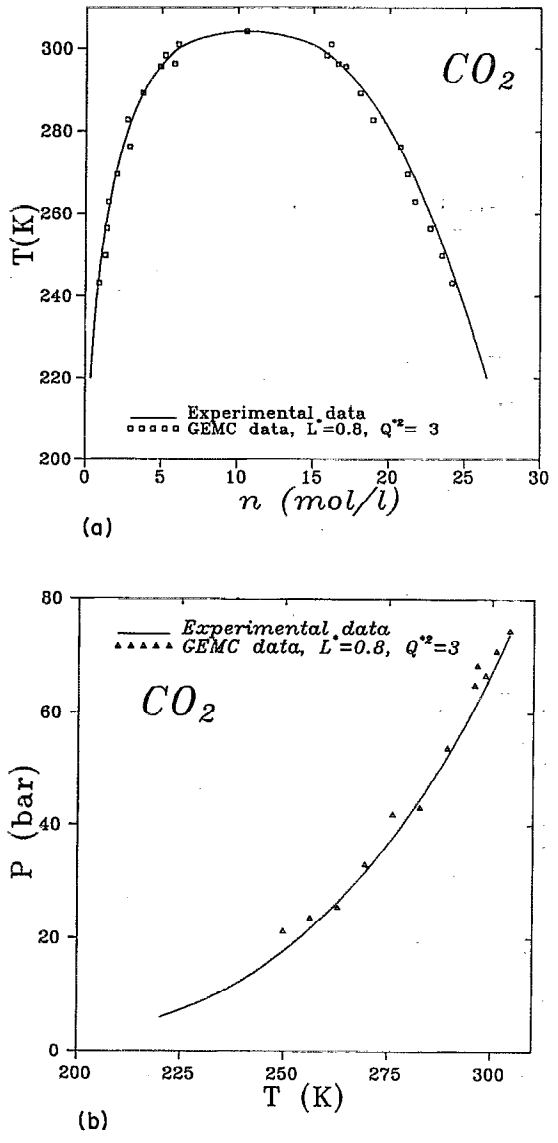

FIG. 10. (a) Vapor–liquid coexistence densities of CO_2. (b) Vapor pressures of CO_2. Solid lines are fittings of experimental data (taken from Ref. 53). Symbols correspond to the simulation data of $L^*=0.8$ and $Q^{*2}=3$, with the parameters obtained as described in the text.

ment obtained from this set of parameters is $Q=4.64\times10^{-26}$ esu cm^2, which in fair agreement with the experimental value,[10] $Q^{exp}=4.3\times10^{-26}$ esu cm^2.

Experimental and simulation coexistence curve and vapor pressures of CO_2 are shown in Fig. 10. We have obtained a very good description of coexistence properties of this fluid by using a simple model for its interaction energy. Therefore, we can conclude that the interaction potential of Eqs. (1)–(3) is a good effective pair potential for the thermodynamic description of a quadrupolar fluid, as carbon dioxide. Möller has also given a good description of thermodynamic and coexistence properties of CO_2 with computer simulations of a quadrupolar two-center Lennard-Jones model.[54] This suggests the possibility of obtaining VLE of any real substance by using the GEMC simulation method. However, this technique is very time consuming. For practical applications, either thermodynamic perturbation theory or integral equations would be desirable. Unfortunately, further work on this area is still needed, although some recent progress has been reported.[20,22,26,28–30,55]

We can estimate from our simulations the critical properties of a hypothetical fluid that would have the same molecular elongation than carbon dioxide, but a quadrupole moment $Q=0$. Its critical temperature, density and pressure would be $T_c=250.31$ K, $n_c=9.75$ mol/l, and $P_c=57.86$ bar. By comparing these values with the actual critical properties of CO_2, we can affirm that quadrupolar interactions increase the critical temperature of real carbon dioxide by about 60 K, the critical density 0.7 mol/l, and the critical pressure about 16 bar. This illustrates what can be learned from computer simulations of fluids models. On the other hand, statistical errors make unclear the influence of molecular elongation and quadrupole on critical compressibility factor.

IV. CONCLUSIONS

We have presented simulations results of vapor–liquid coexistence curves for quadrupolar linear Kihara fluids. To determine VLE, we used the Gibbs ensemble simulation technique. In a previous work,[25] we obtained data of vapor–liquid equilibria for the nonpolar Kihara fluid, and the effect of molecular anisotropy on the coexistence properties was studied, as well as its influence on the departures from the principle of corresponding states.

Here we have shown that the quadrupole moment significantly raises the critical temperature of a molecular fluid. Critical density is raised too, but the increase is smaller. Critical pressure is also increased. Vapor pressure at a given temperature of a linear fluid is decreased by the quadrupole.

We suggest that a more adequate way of reducing the quadrupole moment may be achieved by using the molecular volume. Thus, comparison between properties of quadrupolar fluids of different anisotropy could be easier. We have shown the "universal" behavior of the increase on critical temperature and packing fraction with the quadrupole moment when the *reduced density of quadrupole* is used. The use of this *reduced density of quadrupole* allows us to predict the increase of critical properties by the quadrupole moment and allows an approximate extension of the principle of corresponding states for quadrupolar molecular fluids.

In terms of corresponding states, we have seen that coexistence curve is slightly broadened by the presence of the quadrupole. Same effect was previously found for quadrupolar Lennard-Jones fluids.[15,16] Simulation results indicate that the vapor enthalpy, related with the slope of a $\ln P$ vs $1/T$ plot, is increased by the quadrupole moment.

Influence of shape and quadrupole upon deviations from the principle of corresponding states has also been shown by using plots of $\ln P/P_c$ vs T_c/T. The slope of this plot is related with the *acentric factor*, which has been calculated for all the simulated systems. We found that both shape and quadrupole increase the value of ω.

Finally, we have made use of one of the coexistence curves obtained with GEMC to describe the VLE of carbon dioxide, just by fitting the potential parameters to the critical

temperature and density of real CO_2. We have obtained very good agreement between experiment and simulation data for densities and vapor pressures. This confirms the fact that the quadrupolar Kihara potential constitutes a reliable effective pair potential for real fluids. As a bonus, we have learned the magnitude of the contribution of Q to the critical properties of CO_2. We have illustrated how to use Gibbs ensemble results to determine potential parameters of real substances.

These simulation results can be very useful to test theories of polar molecular fluids, as the perturbation theory presented recently by Boublík.[28–30]

A similar study of linear dipolar Kihara fluids is in progress.

ACKNOWLEDGMENTS

This work was financially supported by project Nos. PB91-0364 and PB91-0602 of the Spanish DGICYT (Dirección General de Investigación Científica y Técnica). One of us (B.G.) wishes to thank a grant of the Universidad Complutense de Madrid to prepare his Ph.D. We are also grateful to the Plan Andaluz de Investigación de la Junta de Andalucía.

[1] K. S. Pitzer, J. Am. Chem. Soc. **77**, 3427 (1955).
[2] E. A. Guggenheim, J. Chem. Phys. **13**, 253 (1945).
[3] R. C. Reid, J. M. Prausnitz, and B. E. Poling, *The Properties of Gases and Liquids* (McGraw–Hill, New York, 1986).
[4] K. S. Pitzer, D. Z. Lippmann, R. F. Curl, C. M. Huggins, and D. E. Peterson, J. Am. Chem. Soc. **77**, 3433 (1955).
[5] D. Cook and J. S. Rowlinson, Proc. Soc. R. Soc. A **219**, 405 (1953).
[6] J. A. Pople, Proc. Soc. R. Soc. A **221**, 498 (1954).
[7] K. E. Gubbins and C. G. Gray, Mol. Phys. **23**, 187 (1972).
[8] G. Stell, J. C. Rasaiah, and H. Narang, Mol. Phys. **23**, 393 (1972).
[9] G. Stell, J. C. Rasaiah, and H. Narang, Mol. Phys. **27**, 1395 (1974).
[10] C. G. Gray and K. E. Gubbins, *Theory of Molecular Fluids* (Clarendon, Oxford, 1984).
[11] L. Verlet and J.-J. Weiss, Mol. Phys. **28**, 665 (1974).
[12] G. N. Patey and J. P. Valleau, J. Chem. Phys. **61**, 534 (1974).
[13] K. S. Shing and K. E. Gubbins, Mol. Phys. **45**, 129 (1982).
[14] D. Levesque, J.-J. Weiss, and G. N. Patey, Mol. Phys. **51**, 333 (1984).
[15] M. P. Stapleton, D. J. Tildesley, A. Z. Panagiotopoulos, and N. Quirke, Mol. Simul. **2**, 147 (1989).
[16] B. Smit and C. P. Williams, J. Phys. Condensed Matter **2**, 4281 (1990).
[17] B. Smit, C. P. Williams, E. M. Hendriks, and S. M. de Leew, Mol. Phys. **68**, 765 (1989).
[18] M. E. van Leeuwen, B. Smit, and E. M. Hendriks, Mol. Phys. **78**, 271 (1993).
[19] P. A. Monson, Mol. Phys. **53**, 1209 (1984).
[20] D. B. Mc Guigan, M. Lupkowski, D. M. Pacquet, and P. A. Monson, Mol. Phys. **67**, 33 (1989).
[21] J. Fischer, R. Lustig, M. Breitenfelder-Manske, and W. Lemming, Mol. Phys. **52**, 485 (1984).
[22] C. Vega and S. Lago, Chem. Phys. Lett. **185**, 516 (1991).
[23] E. de Miguel, L. F. Rull, M. K. Chalam, and K. E. Gubbins, Mol. Phys. **71**, 1223 (1990).
[24] E. de Miguel, L. F. Rull, and K. E. Gubbins, Physica A **177**, 174 (1991).
[25] C. Vega, S. Lago, E. de Miguel, and L. F. Rull, J. Phys. Chem. **96**, 7431 (1993).
[26] M. Lupkowski and P. A. Monson, Mol. Phys. **67**, 53 (1989).
[27] G. S. Dubey, S. F. O'Shea, and P. A. Monson, Mol. Phys. **80**, 997 (1993).
[28] T. Boublík, Mol. Phys. **73**, 417 (1991).
[29] T. Boublík, Mol. Phys. **76**, 327 (1992).
[30] T. Boublík, Mol. Phys. **77**, 983 (1992).
[31] T. Kihara, J. Phys. Soc. Jpn. **16**, 289 (1951).
[32] T. Kihara, Chem. Phys. Lett. **92**, 175 (1982).
[33] T. Kihara and A. Koide, Adv. Chem. Phys. **33**, 51 (1975).
[34] T. Boublík, J. Chem. Phys. **87**, 1751 (1987).
[35] P. Padilla, S. Lago, and C. Vega, Mol. Phys. **74**, 161 (1991).
[36] C. Vega and S. Lago, J. Chem. Phys. **94**, 310 (1991).
[37] C. Vega, S. Lago, and P. Padilla, J. Phys. Chem. **96**, 1900 (1992).
[38] C. Vega and S. Lago, J. Chem. Phys. **93**, 8171 (1990).
[39] C. Vega, *Termodinámica Estadística del Estado Líquido*, Ph.D. thesis, Universidad Complutense de Madrid, 1991.
[40] P. Sevilla and S. Lago, Comput. Chem. **9**, 39 (1985).
[41] S. Lago and C. Vega, Comput. Chem. **12**, 343 (1988).
[42] S. Lago and C. Vega, Comput. Chem. **18**, 55 (1994).
[43] A. Z. Panagiotopoulos, Mol. Phys. **61**, 813 (1987).
[44] A. Z. Panagiotopoulos, N. Quirke, M. Stapleton, and D. J. Tildesley, Mol. Phys. **63**, 527 (1988).
[45] C. Vega and D. Frenkel, Mol. Phys. **67**, 633 (1989).
[46] M. Bohn, J. Fischer, and J. M. Haile, Mol. Phys. **65**, 797 (1988).
[47] C. Vega and K. E. Gubbins, Mol. Phys. **72**, 881 (1992).
[48] P. Pfeuty and G. Toulose, *Introduction to the Renormalization Group and to Critical Phenomena* (Wiley, New York, 1977).
[49] I. M. Klotz and R. M. Rosenberg, *Chemical Thermodynamics* (Benjamin, Menlo Park, CA, 1986).
[50] A. Lotfi, O. Vrabec, and J. Fischer, Mol. Phys. **76**, 1319 (1992).
[51] L. Pauling, *General Chemistry*, 3rd ed. (Freeman, San Francisco, 1970).
[52] P. W. Atkins and J. A. Beran, *General Chemistry* (Scientific America Library, New York, 1992).
[53] S. Angus, B. Armstrong, and K. M. de Reuck, *International Thermodynamic Tables of Fluid Carbon Dioxide* (IUPAC, Pergamon, 1973).
[54] D. Möller, *Thermodynamik Fluider Mischungen: Kalorimetrie und Computersimulationen*, Ph.D. thesis, Bochum, 1991.
[55] A. L. Benavides, Y. Guevara, and F. del Río, Physica A **202**, 420 (1993).